Journal of the Optical Society of Korea
Vol. 20, No. 3, June 2016, pp. 401-406

ISSN: 1226-4776(Print) / ISSN: 2093-6885(Online)
DOI: http://dx.doi.org/10.3807/JOSK.2016.20.3.401

Performance Enhancement of Cavity Assisted Photonic Crystal De-Multiplexer in Slow Light Regime

Mohammad-Hashem Vadjed-Samiei* and Hassan Aghababaeian

Faculty of Electrical Engineering, Iran University of Science and Technology, Tehran, Iran

(Received January 18, 2016 : revised May 25, 2016 : accepted May 26, 2016)

This study first proposes a new version of a photonic crystal based de-multiplexer operating under the slow light regime, secondly analyses the structure numerically to demonstrate de-multiplexing operation and finally studies the impact of light speed on the performance of the proposed structure. The operation wavelength is 1.55 μm. The study indicates that, by adjusting the speed of light, around 0.1C, in the main waveguide and in the output channels' waveguides, an enhancement in the performance of the de-multiplexer will be gained.

Keywords : Photonic crystal, Slow light, Optical de-multiplexer
OCIS codes : (130.3120) Integrated optics devices; (060.1810) Buffers, couplers, routers, switches, and multiplexers

I. INTRODUCTION

The advent of the wavelength division multiplexing (WDM) technique around 1992 started a revolution in optical fiber transmission systems. In order to use the maximum transmission capacity of optical fibers and to maximize optical networks' throughputs to their maximum possible values, designers should rely on high speed, low loss, low power consumption and compact alloptical components [1]. These components are vitally important to design and fabricate complex and efficient terminal equipment. Photonic waveguides and photonic crystal waveguides (PCW) are two competing available optical component design platforms. Integration is another technical possibility with its own advantages, compatible with the above-mentioned requirements.

One of the key WDM components is the De-multiplexer (DEMUX), which is characterized by the number and selectivity of it output channels. Some photonic waveguide based DEMUX designs are reported by researchers [1-6]. Because of their weak optical confinement, these components are not of interest of the researchers, whereas more compact designs are possible based on photonic crystal technology [7, 8]. Photonic crystal (PhC) based DEMUX designs are superior in this respect [7-11]. Various methods are proposed by researchers to provide the required frequency selectivity of the output channels. Whilst directional coupler based selectivity has been used in [12-14], resonator based selectivity has been proposed in [7, 15, 16], using cavity, line and ring resonators. Channel bandwidths of the directional coupler based designs are wider than their resonator based counterparts.

Decreasing the group velocity of light leads to enhancement of the wavematter interaction which may be used to improve performances of optical components [18-20]. Photonic crystal waveguide is a suitable medium to control the speed of light and hence is a relevant platform to design slow light based photonic devices [18-20]. In this study we consider the impact of slow light technology on the photonic crystal based DEMUX. In a design reported in 2011 a compact wavelength DEMUX using cascaded single mode PCW utilizing the slow light regime waspropose[21]. That design is based on a near band-edge slow light operating point, resulting in a large value of group velocity dispersion (GVD).

The effects of light speed on the performance of PC DEMUXs have not yet been considered in the previous studies. This study, firstly proposes a PhC based DEMUX, consisting of a main waveguide and cavity coupled output

*Corresponding author: mh_samiei@iust.ac.ir
Color versions of one or more of the figures in this paper are available online.

channels under a slow light regime, secondly analyses the structure numerically to demonstrate de-multiplexing operation and finally studies the impact of light speed on the performance of the proposed structure. The remainder of the paper is organized as follows: Section II considers the structure of the proposed DEMUX, its operation principles and design considerations based on a series of relevant numerical simulations. The effects of the speed of light on performance of the proposed structure are also studied in Section II. Section III is devoted to discussion and conclusions.

II. DESIGNING A PHOTONIC CRYSTAL SLOW LIGHT BASED DEMUX

The proposed design consists of a main waveguide carrying input channels, $\lambda_1,\lambda_2,\cdots,\lambda_n$, and n side-coupled cavity-assisted output channels (λ_i, i=1 to n) embedded in a square lattice photonic crystal medium. Figure 1 shows schematically the four channels DEMUX under study, in Fig. 1(a), and details of one of its units, in Fig. 1(b). Using the scalability property of PhCs and their derived structures, each unit of the DEMUX is designed to function selectively on one of the DEMUX output channel wavelengths. All waveguides, the main one and the output channel waveguides, are designed considering the slow light regime in their operating wavelength bands. The wavelength band in the main PCW should be wide enough to cover all input channels. Some wideband slow light PCW designs have been reported in the literature [22-25]. Generally in these designs the PCW is formed by removal of a row of PhC elements and the slow light regime of operation is established by modification of PhC elements of the two first rows in each side wall of the PCW. As in our DEMUX design the output channels are coupled to the main PCW through side coupled cavities, these modified rows will degrade the selective performance of the cavities and their related output channels. In our proposed DEMUX design both input channels' guidance and wideband slow light performance of the main PCW is based on a line defect in which the elements are narrower than the regular elements of the hosting photonic crystal medium.

The plane wave expansion method, PWE, is the method of choice to find the dispersion diagram of PCWs, although other methods such as FDTD, FEM, …are used too. In our study we have used the PWE method and selecting an appropriate supercell using MIT photonic band (MPB) package [26] along with Bandsolve tools of Rsoft package [27]. The dispersion curve of the PCW should be located inside the

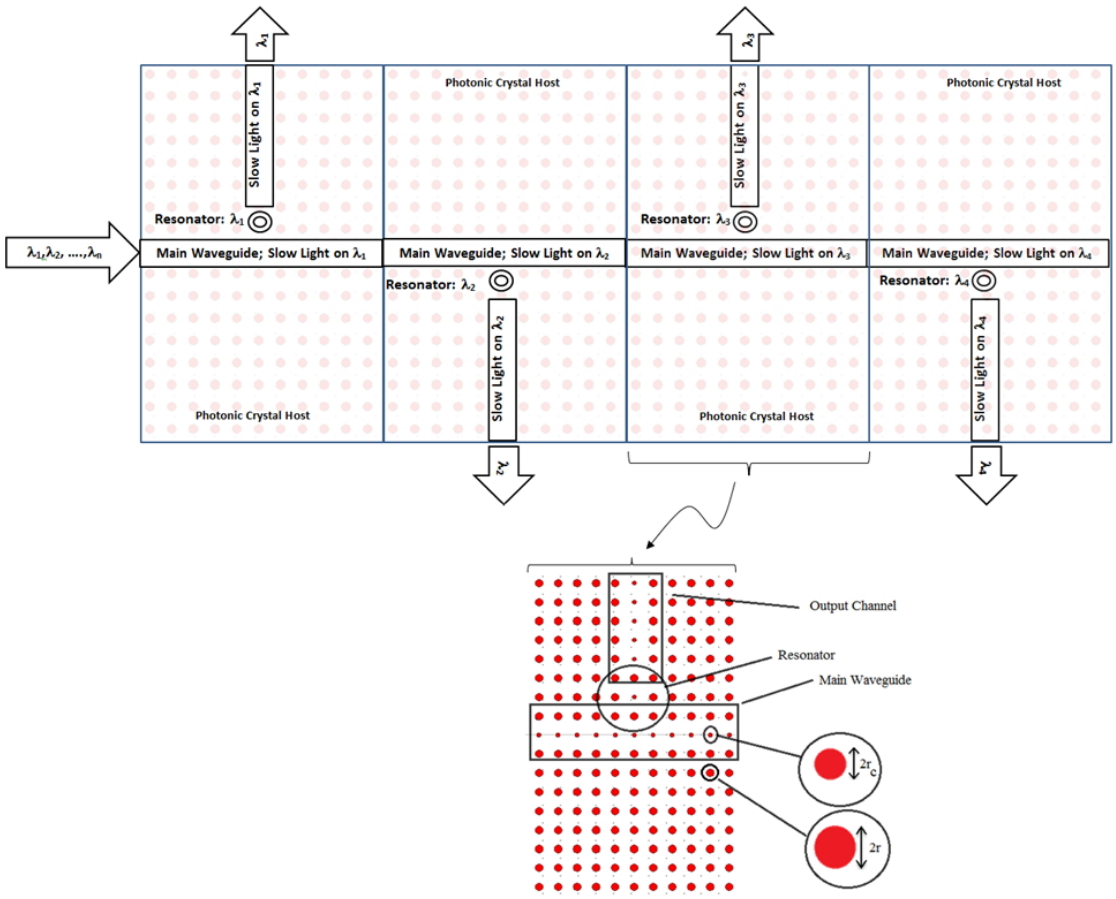

FIG. 1. Slow light based photonic crystal DEMUX. (a) general view of signal flow in DEMUX, (b) a typical unit of DEMUX consisting of the main slow light PCW, side coupled cavity and slow light output channel.

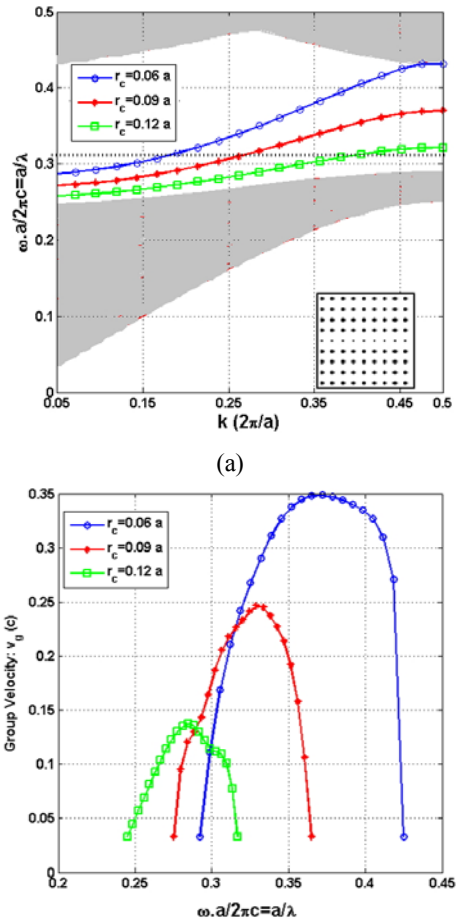

FIG. 2. Slow light PCW created by reducing the radii of a row of rods (r_c) in a square lattice of photonic crystal (inset). (a) Dispersion diagram of the TM mode in PCW for three different values of r_c. (b) Related group velocity for three different values of r_c.

bandgap of the hosting photonic crystal. The proposed photonic crystal structure exhibits a bandgap only for TM polarization. The resulting dispersion diagram for the TM mode of the main PCW of the Fig. 1 is shown in Fig. 2(a) for three values of r_c. Simulation parameters are: $n_{si}=3.46$ (refractive index of silicon), a=500 nm and r=0.185a (lattice constant and rods radii of the square photonic crystal respectively). These values for structural parameters of the photonic crystal correspond to a wavelength range of λ=1.28 μm (against a/λ=0.42) to λ=1.86 μm (against a/λ=0.29) for the PBG, covering two optical communication windows of 1.3 μm and 1.55 μm.

As it is indicated in the Fig. 2(a) the slope of the dispersion curves of the TM propagation modes depend on the radii of central rods of the PCW (r_c). In the Fig. 2(b) curves of variations of group velocity normalized to the speed of the light in free space, $c\left(\frac{1}{c}v_g=\frac{1}{c}d\omega/dk\right)$ against the normalized frequency ($\omega\cdot a/2\pi c=a/\lambda$) for three values

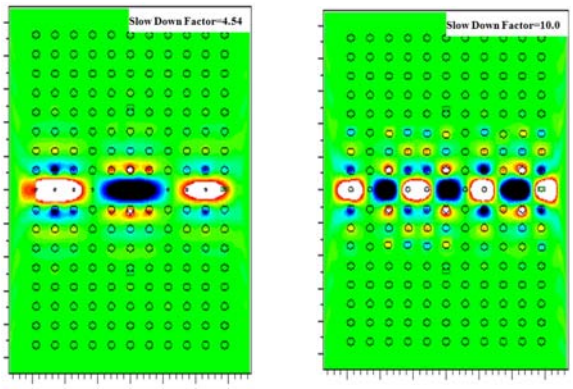

FIG. 3. Electric field distribution of the TM propagating mode with normalized frequency of a/λ=0.313 in the studied PCW for (a) r_c/a=0.06 and (b) r_c/a=0.12 which corresponds to v_g= 0.22c and v_g=0.1c (slow down factors of 4.54 and 10.0, respectively).

of r_c (0.06a, 0.09a and 0.12a) are indicated. The vertical axis of the figure indicates the normalized group velocity of v_g/c. For a given value of r_c, a range of values for the normalized group velocity is attainable, depending on the value of a/λ. For example for r_c=0.06a, the attainable normalized group velocity in the bandgap (a/λ=0.29 to a/λ=0.42), is in the range of 0.04 to 0.35. On the other hand, for a given value of wavelength (or a/λ) a range of values for normalized group velocity is attainable depending on the values of r_c. For example, for a/λ=0.313, normalized group velocity of 0.22 and 0.1 are attainable corresponding to r_c=0.06a and r_c=0.12a respectively

Figure 3 shows the electric field distribution of the TM propagating mode of the PCW for two different slowdown factors of c/v_g=4.54($v_g/c=0.22$) and c/v_g=10($v_g/c=0.10$) corresponding to r_c/a=0.06 and r_c/a=0.12, respectively, at normalized frequency of a/λ=0.313. These figures have been obtained using Rsoft Fullwave package [28] which is based on the FDTD simulation method. As it is expected the figure indicates that increasing the slowdown factor leads to spatial compression of the propagating mode in the longitudinal direction and more field penetration in the transversal direction. This effect may be used to design a new class of photonic crystal devices [19, 20, 21], namely slow light devices, including the DEMUX design of our study.

In the design under study, this integration finally will lead to an enhancement of energy transfer from the main PCW to output channels. In Fig. 4, the relation of the main PCW and one of the output channels is indicated. Selectivity of energy transfer is due to selectivity of slow light operation of the main PCW in the coupling region, inherent selectivity of the side coupled cavity and selective slow light operation of the output channel, all on the assigned output wavelength. Figure 4(a) and Fig. 4(b) repeat the field distribution of Fig. 3 with the same parameters

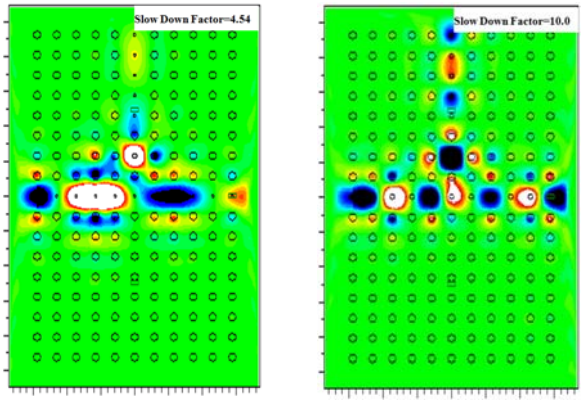

(a) (b)

FIG. 4. Electric field distribution of the TM mode de-multiplexed at normalized frequency of a/λ= 0.313 for two slow down factors of 4.54 and 10.0 (r_c/a=0.06 and r_c/a=0.12, respectively).

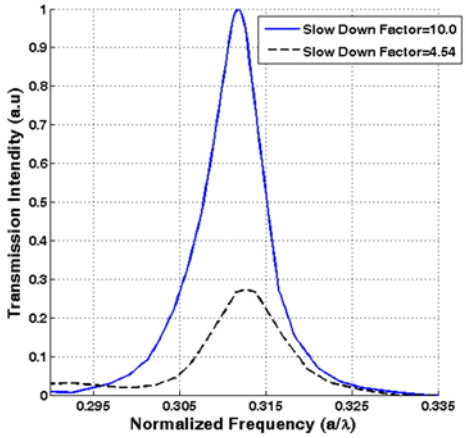

FIG. 5. Frequency spectrum of the output channels in two slow down factors of 4.54 and 10.0 (r_c/a=0.06 and r_c/a=0.12, respectively).

considering one of the output channels on wavelength of λ_i ($\lambda_i=a/0.313$ in this case that is tuned if $r_{cav}=0.07r$ is to be considered for the radius of the side cavity).

A Gaussian optical pulse, covering the whole frequency-range-of-interest, is launched at the input of the main waveguide. Power monitors were placed at the output channel to collect the transmitted spectral power density. The transmitted spectral power densities were normalized to the incident light spectral power density from the input port. Figure 5 shows the transmission coefficient of the output channel against normalized frequency (a/λ) in the range of 0.290 to 0.335, for slowdown factor of 4.54 to 10. The figure confirms the selective energy transfer enhancement due to slow light based design.

The same principle of operation is applied to all channels of DEMUX under study. Designing parameters of the DEMUX, using scalability of PhCs and their derived structures are

TABLE 1. Designing parameters of four channels DEMUX

Channel No.	a Lattice Constant (nm)	r_{cav} Cavity Radius (nm)	a/λ Norm. Dropped Freq.	λ (nm) Dropped Wavelength
1	500	6.50	0.313	1597
2	490	6.35	0.313	1565
3	480	6.20	0.313	1533
4	470	6.05	0.313	1502

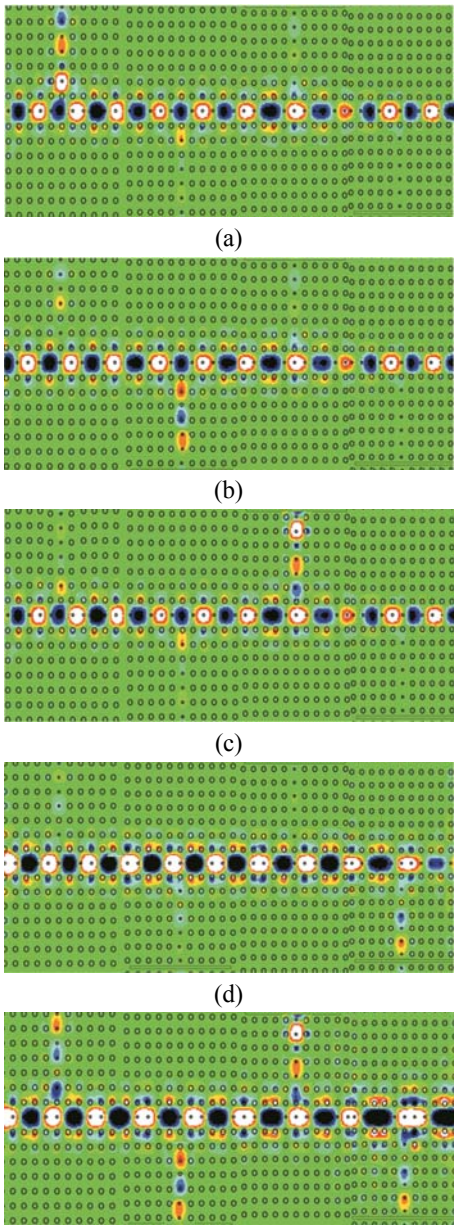

(a) (b) (c) (d) (e)

FIG. 6. Electric field distribution of the TM mode in four channel DEMUX with source wavelengths of (a) λ=1.597 μm, (b) λ=1.565 μm, (c) λ=1.533 μm, (d) λ=1.502 μm and (e) full spectrum excitation.

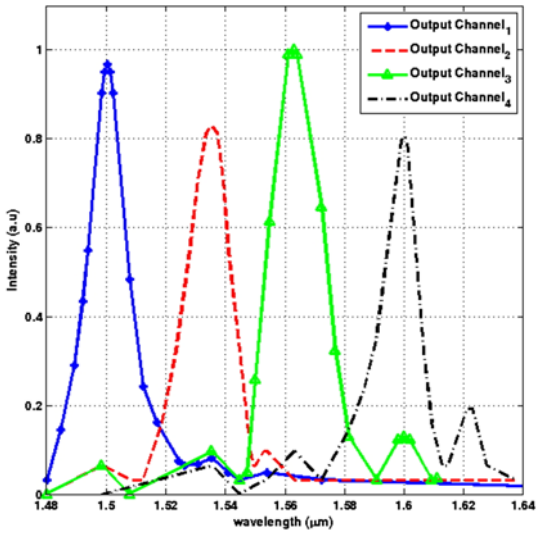

FIG. 7. The normalized transmission spectra of four channel slow light DEMUX.

indicated in Table 1.

Figure 6(a) to 6e indicate electric field distributions in the DEMUX structure under separate channel excitations at λ_1=1.597 μm, λ_2=1.565 μm, λ_3=1.533 μm, λ_4=1.502 μm and under full DEMUX spectrum, λ_1 to λ_4, excitation.

The Fig. 7 shows normalized transmission spectrum of the DEMUX, with a good channel separation (cross talk) and correct channel placement.

III. CONCLUSIONS

This study shows capabilities of slow light to enhance the performance of photonic crystal demultiplexers. The component consists of a main photonic crystal waveguide and side coupled cavity assisted output branches. The signal in each of the de-multiplexer channels, in addition to pass through the selective element of cavity in its path, undergo selectively twice the slow light propagating condition, the first time in the coupling region of the branching point and then in the output channel waveguide. Our study indicates that each of the slow light regions enhances independently the overall frequency spectrum of the de-multiplexer, both in amplitude and channel selectivity aspects.

REFERENCES

1. D. A. B Miller, "Device requirements for optical interconnects to silicon chips," Proc. IEEE **97**, 1166-1185 (2009).
2. R. A. Soref, "Silicon-based optoelectronics," Proc. IEEE **81**, 1687-1706 (1993).
3. P. Yeh and H. F. Taylor, "Contradirectional frequency-selective couplers for guided-wave optics," Appl. Opt. **19**, 2848-2855 (1980).
4. H.-D. Jang, K.-S. Kim, J.-H. Lee, and J.-C. Jeong, "Transmission performance of 40 gb/s pm duobinary signals due to fiber nonlinearities in DWDM systems using VSB filtering techniques," J. Opt. Soc. Korea **13**, 354-360 (2009).
5. D. T. H. Tan, K. Ikeda, S. Zamek, A. Mizrahi, M. P. Nezhad, A. V. Krishnamoorthy, J. E. C. K. Raj, X. Zheng, I. Shubin, Y. Luo, and Y. Fainman, "Wide bandwidth, low loss 1 by 4 wavelength division multiplexer on siliconfor optical interconnects," Opt. Express **19**, 2401-2409 (2011).
6. D. D. Do, J. W. An, N. Kim, and K. Y. Lee, "Gaussian apodization technique in holographic demultiplexer based on photopolymer," J. Opt. Soc. Korea **7**, 269-274 (2003).
7. Z. Qiang, W. Zhou, and R. A. Soref, "Optical add-drop filters based on photonic crystal ring resonators," Opt. Express **15**, 1823-1831 (2007).
8. A. Rostami, F. Nazaria, H. A. Banaei, and A. Bahrami, "A novel proposal for DWDM demultiplexer design using modified-T photonic crystal structure," Photonics Nanostruct. Fundam. Appl. **8**, 14-22 (2010).
9. T. Niemi, L. H. Frandsen, K. K. Hede, A. Harpoth, P. I. Borel, and M. Kristensen, "Wavelength-division demultiplexing using photonic crystal waveguides," IEEE Photon. Technol. Lett. **18**, 226-228 (2006).
10. Y. Wu, K. Hsu and T. Shih, "Thirty-two-channel dense-wavelength-division multiplexer based on cascade two-dimensional photonic crystal waveguide structure," J. Opt. Soc. Am. B **24**, 2075-2080 (2007).
11. H. Benisty, C. Cambournac, F. Van Laere, and D. Van Thourhout, "Photonic-crystal demultiplexer with improved crosstalk by second-order cavity filtering," IEEE J. Lightwave Technol. **28**, 1201-1208 (2010).
12. M. Thorhauge, L. H. Frandsen, and P. I. Borel, "Efficient photonic crystal directional couplers," Opt. Lett. **28**, 1525-1527 (2003).
13. M. Bayindir and E. Ozbay, "Band-dropping via coupled photonic crystal waveguides," Opt. Express **10**, 1279-1284 (2002).
14. F. S.-S. Chien, Y.-J. Hsu, W.-F. Hsieh, and S.-C. Cheng, "Dual wavelength demultiplexing by coupling and decoupling of photonic crystal waveguides," Opt. Express **12**, 1119-1125 (2004).
15. S. Fan, P. R. Villeneuve, J. D. Joannopoulos, and H. A. Haus, "Channel drop filters in photonic crystals," Opt. Express **3**, 4-11 (1998).
16. S. Robinson and R. Nakkeeran, "Photonic crystal ring resonator-based add drop filters: a review," Opt. Eng. **52**, 060901-1~060901-11 (2013).
17. M. D. Settle, R. J. P. Engelen, M. Salib, A. Michaeli, L. Kuipers, and T. F. Krauss, "Flatband slow light in photonic crystals featuring spatial pulse compression and terahertz bandwidth," Opt. Express **15**, 219-226 (2007).
18. T. F. Krauss, "Why do we need slow light," Nature Photon. **2**, 448-450 (2008).
19. J. M. Brosi, "Slow-light photonic crystal devices for high-speed optical signal processing," Karlsruhe Series in Photon. & Comm., vol. 4 (2008).
20. H. Aghababaeian and M. H. Vadjed Samiei, "Compact and temperature independent electro-optic switch based on slotted silicon photonic crystal directional coupler," J. Opt. Soc. Korea **16**, 282-287 (2012).

21. A. Akosman, M. Mutlu, H. Kurt, and E. Ozbay, "Compact wavelength de-multiplexer design using slow light regime of photonic crystal waveguides," Opt. Express **19**, 24129-24138 (2011).
22. T. F. Krauss, "Slow light in photonic crystal waveguides," J. Phys. D: Appl. Phys. **40**, 2666-2670 (2007).
23. T. Baba and D. Mori, "Slow light engineering in photonic crystals," J. Phys. D: Appl. Phys. **40**, 2659-2665 (2007).
24. H. Aghababaeian, M. H. Vadjed-Samiei, and N. Granpayeh, "Temperature stabilization of group index in silicon slotted photonic crystal waveguides," J. Opt. Soc. Korea **15**, 398-402 (2011).
25. A. Y. Petrov and M. Eich, "Zero dispersion at small group velocities in photonic crystal waveguides," Appl. Phys. Lett. **85**, 4866-4868 (2004).
26. http://ab-initio.mit.edu/wiki/index.php/MIT_Photonic_Bands
27. http://optics.synopsys.com/rsoft/rsoft-passive-device-bandsolve.html
28. http://optics.synopsys.com/rsoft/rsoft-passive-device-fullwave.html